

See discussions, stats, and author profiles for this publication at: <https://www.researchgate.net/publication/263208421>

An Elusive Hydridoaluminum(I) Complex for Facile C–H and C–O Bond Activation of Ethers and Access to Its Isolable Hydridogallium(I) Analogue: Syntheses, Structures, and Theoretical...

ARTICLE *in* JOURNAL OF THE AMERICAN CHEMICAL SOCIETY · JUNE 2014

Impact Factor: 12.11 · DOI: 10.1021/ja504448v · Source: PubMed

CITATIONS

5

READS

66

5 AUTHORS, INCLUDING:



Gengwen Tan

Technische Universität Berlin

18 PUBLICATIONS 175 CITATIONS

SEE PROFILE



Burgert Blom

Maastricht University

51 PUBLICATIONS 330 CITATIONS

SEE PROFILE

An Elusive Hydridoaluminum(I) Complex for Facile C–H and C–O Bond Activation of Ethers and Access to Its Isolable Hydridogallium(I) Analogue: Syntheses, Structures, and Theoretical Studies

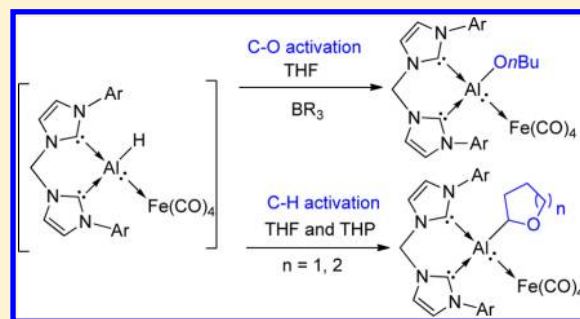
Gengwen Tan,[†] Tibor Szilvási,[‡] Shigeyoshi Inoue,[†] Burgert Blom,[†] and Matthias Driess^{*,†}

[†]Department of Chemistry: Metalorganics and Inorganic Materials, Sekr. C2, Technische Universität Berlin, Strasse des 17. Juni 135, 10623 Berlin, Germany

[‡]Department of Inorganic and Analytical Chemistry, Budapest University of Technology and Economics, Szent Gellért tér 4, 1111 Budapest, Hungary

S Supporting Information

ABSTRACT: The reaction of AlBr_3 with 1 molar equiv of the chelating bis(*N*-heterocyclic carbene) ligand bis(*N*-Dipp-imidazole-2-ylidene)methylene (bisNHC, **1**) affords $[(\text{bisNHC})\text{AlBr}_2]^+\text{Br}^-$ (**2**) as an ion pair in high yield, representing the first example of a bisNHC–Al(III) complex. Debromination of the latter with 1 molar equiv of $\text{K}_2\text{Fe}(\text{CO})_4$ in tetrahydrofuran (THF) furnishes smoothly, in a redox reaction, the $(\text{bisNHC})(\text{Br})\text{Al}[\text{Fe}(\text{CO})_4]$ complex **3**, in which the Al(I) center is stabilized by the $\text{Fe}(\text{CO})_4$ moiety through Al(I): \rightarrow Fe(0) coordination. Strikingly, the Br/H ligand exchange reactions of **3** using potassium hydride as a hydride source in THF or tetrahydropyran (THP) do not yield the anticipated hydridoaluminum(I) complex $(\text{bisNHC})\text{Al}(\text{H})[\text{Fe}(\text{CO})_4]$ (**4a**) but instead lead to $(\text{bisNHC})\text{Al}(2\text{-cyclo-OC}_4\text{H}_7)[\text{Fe}(\text{CO})_4]$ (**4**) and $(\text{bisNHC})\text{Al}(2\text{-cyclo-OC}_5\text{H}_9)[\text{Fe}(\text{CO})_4]$ (**5**), respectively. The latter are generated via C–H bond activation at the α -carbon positions of THF and THP, respectively, in good yields with concomitant elimination of dihydrogen. This is the first example whereby a low-valent main-group hydrido complex facilitates metalation of sp^3 C–H bonds. Interestingly, when $\text{K}[\text{BHR}_3]$ ($\text{R} = \text{Et}, \text{sBu}$) is employed as a hydride source to react with **3** in THF, the reaction affords $(\text{bisNHC})\text{Al}(\text{OnBu})[\text{Fe}(\text{CO})_4]$ (**6**) as the sole product through C–O bond activation and ring opening of THF. The mechanisms for these novel C–H and C–O bond activations mediated by the elusive hydridoaluminum(I) complex **4a** were elucidated by density functional theory (DFT) calculations. In contrast, the analogous hydridogallium(I) complex $(\text{bisNHC})\text{Ga}(\text{H})[\text{Fe}(\text{CO})_4]$ (**9**) can be obtained directly in high yield by the reaction of the $(\text{bisNHC})\text{Ga}(\text{Cl})[\text{Fe}(\text{CO})_4]$ precursor **8** with 1 molar equiv of $\text{K}[\text{BHR}_3]$ ($\text{R} = \text{Et}, \text{sBu}$) in THF at room temperature. The isolation of **9** and its inertness toward cyclic ethers might be attributed to the higher electronegativity of gallium versus aluminum. The stronger Ga(I)–H bond, in turn, hampers α -C–H metalation or C–O bond cleavage in cyclic ethers, the latter of which is supported by DFT calculations.



INTRODUCTION

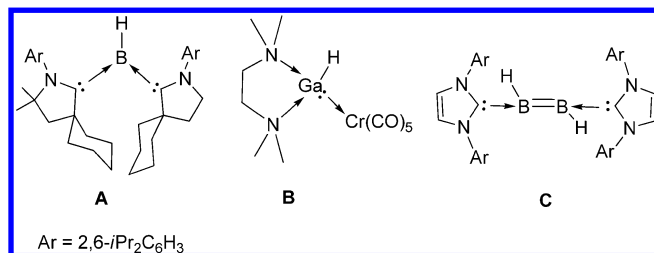
Low-valent main-group chemistry continues to represent a highly attractive research frontier in contemporary organometallic chemistry, partially because of the pursuit of transition-metal-free small-molecule activation reactions and transformations.¹ Low-valent main-group metal hydrides of the group 13, 14, and 15 elements are of interest since they have already shown some potential in the hydrogenation of unsaturated substrates such as alkynes, ketones, and imines as well as carbon dioxide, either stoichiometrically or catalytically.^{1d,2} However, these parent metal hydrides (e.g., AlH_3 , SnH_2 , etc.) are highly reactive because of the lack of steric protection. To date, tremendous efforts have been undertaken in synthesizing divalent group 14 metal hydrides (EH_2 , $\text{E} = \text{Si-Pb}$), and dozens of complexes stabilized by sterically demanding ligands R in REH ($\text{E} = \text{Si-Pb}$) or through Lewis-

type donor–acceptor stabilization have been reported.^{2b,3} In comparison to the flourishing divalent group 14 (semi)metal hydride chemistry, the field for low-valent group 13 elements is far less developed.⁴ The stabilization of “free” $\text{Al(I)}\text{–H}$ and $\text{Ga(I)}\text{–H}$ species has been spectroscopically studied by matrix isolation techniques at low temperatures through the reactions of elemental aluminum and gallium, respectively, with dihydrogen under UV-light irradiation.⁵ These species are extremely reactive and tend to react readily with another equivalent of dihydrogen to form the corresponding metal trihydrides at elevated temperatures. However, isolable monovalent group 13 (semi)metal hydride complexes are exceptionally scarce. The only existing examples reported to

Received: May 4, 2014

date are (CAAC)₂BH **A** [CAAC = cyclic (alkyl)(amino)-carbene] and (TMEDA)Ga(H)[Cr(CO)₅] **B** (TMEDA = *N,N'*-tetramethylethylenediamine) reported by Bertrand and co-workers⁶ and Fischer et al.,⁷ respectively (Chart 1). The

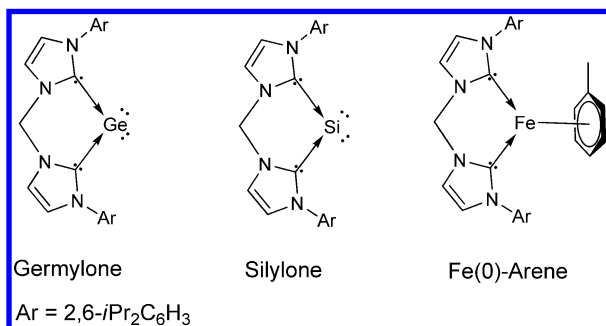
Chart 1. Known Hydridoelement(I) Complexes of the Group 13 Elements



hydridoboron(I) moiety in **A** is stabilized by two neutral carbene ligands, whereas the Ga(I)–H moiety in **B** is stabilized by TMEDA and a Cr(CO)₅ moiety acting as an electron donor and acceptor, respectively. Additionally, Robinson and co-workers reported the N-heterocyclic carbene (NHC)-stabilized diborene complex **C**, which can be described as a dimer of (NHC)BH.⁸ Until now, Al(I)–H and complexes thereof have still escaped isolation. Considering this early stage in the development in low-valent group 13 metal hydride chemistry, it would be desirable to extend the chemistry with more ligand scaffolds in an attempt to garner more structural and reactivity properties.

We recently demonstrated that the chelating ligand bis(*N*-Dipp-imidazole-2-ylidene)methylene (bisNHC, **1**) (Dipp = 2,6-diisopropylphenyl) can serve as very sufficient supporting ligand to stabilize low-valent metal complexes: germylone⁹ and silylone¹⁰ [divalent germanium(0) and silicon(0) compounds that feature two lone pairs of electrons at the respective element sites]¹¹ as well as Fe(0)–arene complexes¹² could be prepared (Chart 2). Moreover, several Fe(II) complexes

Chart 2. Low-Valent (Semi)Metal Complexes Stabilized by bisNHC Ligand **1**



supported by this ligand have also been reported by Ingleson and co-workers¹³ and Meyer et al.¹⁴ Inspired by these results, we were interested in obtaining hydridoaluminum(I) and hydridogallium(I) complexes employing the bisNHC ligand.

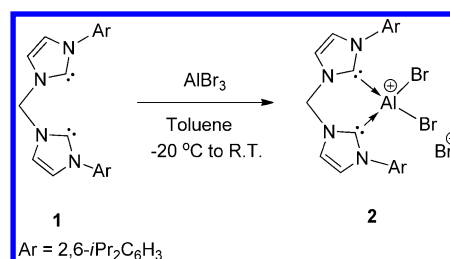
Herein we report the synthesis of the elusive (bisNHC)Al(H):→[Fe(CO)₄] complex **4a** and its isolable Ga(I) analogue (bisNHC)Ga(H):→[Fe(CO)₄] (**9**), which show distinctly different reactivities. While compound **4a** enables unexpectedly facile C–H and C–O bond activation of tetrahydrofuran (THF) and tetrahydropyran (THP), complex **9** is inert toward

ethers and can be isolated in high yields. THF and THP molecules are deprotonated by **4a** at the α -carbon positions to yield (bisNHC)Al(2-*cyclo*-OC₄H₇)[Fe(CO)₄] (**4**) and (bisNHC)Al(2-*cyclo*-OC₅H₉)[Fe(CO)₄] (**5**), respectively, with concomitant elimination of dihydrogen. To the best of our knowledge, this represents the first example of deprotonation of sp³ C–H bonds with a low-valent main-group hydride complex. In the former case, the C–O bond in THF can be cleaved with concomitant ring opening to afford (bisNHC)Al(OnBu)[Fe(CO)₄] (**6**) as the sole product. The reaction mechanisms for both C–H and C–O bond activations have been elucidated by density functional theory (DFT) calculations.

RESULTS AND DISCUSSION

We first synthesized the precursor [(bisNHC)AlBr₂]⁺Br[−] (**2**) by treatment of bisNHC **1** with 1 molar equiv of AlBr₃ in toluene (Scheme 1). Compound **2** was isolated as an off-white

Scheme 1. Synthesis of the Precursor [(bisNHC)AlBr₂]⁺Br[−] (2**)**



solid in high yield (92%) and represents the first example of any aluminum trihalide complex stabilized by a chelating bis(N-heterocyclic carbene) ligand. It is noteworthy that the reaction of an ethylene-bridged bis(N-heterocyclic carbene) ligand with AlCl₃ led to the isolation of the bis(imidazolium) salt as reported by Jones and co-workers,¹⁵ and mono-NHC-stabilized AlX₃ (X = Cl, I) has been reported by Roesky and co-workers.¹⁶ Very recently, a tetracarbene-supported Al(III) complex has also been reported.¹⁷

The solid-state structure of **2** was unambiguously determined by single-crystal X-ray diffraction analysis, which revealed that **2** is an ion pair with a bromide counteranion (Figure 1). The aluminum center features a tetrahedral geometry with the coordination of two carbon atoms from the bisNHC ligand and

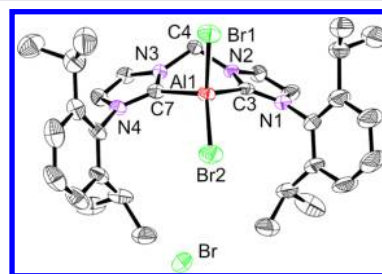
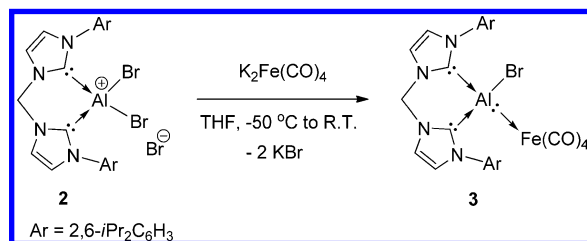


Figure 1. Solid-state structure of complex **2.** Thermal ellipsoids are drawn at the 50% probability level, and all of the H atoms and the solvent molecule have been omitted for clarity. Selected bond lengths (Å) and angles (deg): Al1–C3 2.027(5), Al1–C7 2.018(5), Al1–Br1 2.2708(15), Al1–Br2 2.2611(15); C3–Al1–C7 93.7(2), C3–Al1–Br2 116.96(15), C3–Al1–Br1 109.63(14), C7–Al1–Br2 114.05(15), C7–Al1–Br1 108.83(15), Br1–Al1–Br2 112.13(6).

two bromine atoms. The Al–C bond distances [2.018(5) and 2.027(5) Å] are similar to the bond distance of 2.031(2) Å in $(\text{IPr})\text{AlI}_3$ [$\text{IPr} = :C(\text{ArNCH})_2$, $\text{Ar} = 2,6\text{-iPr}_2\text{C}_6\text{H}_3$].^{16b} In the asymmetric unit, another molecule of $[(\text{bisNHC})\text{-AlBr}_2]^+[\text{AlBr}_4]^-$ (**2a**) with AlBr_4^- as the counteranion is cocrystallized with **2** (the structure of **2a** is shown in Figure 1s in the Supporting Information). The formation of **2a** is probably due to the slight molar excess of AlBr_3 in the reaction, and if bisNHC **1** is used in a slightly excess amount (1.05 molar equiv with respect to AlBr_3), compound **2** is exclusively formed. In accordance with its ionic nature, compound **2** is soluble in CH_2Cl_2 and acetonitrile but only marginally soluble in nonpolar solvents such as toluene and diethyl ether. The ^1H NMR spectrum in CD_2Cl_2 shows two doublet resonance signals ($\delta = 1.05$ and 1.18 ppm) and one septet signal ($\delta = 2.36$ ppm) for the isopropyl groups, indicating a C_{2v} geometry of the molecule in solution, which is consistent with the structure in the solid state. The protons of the bridging methylene group resonate at $\delta = 7.83$ ppm as a singlet.

With the precursor **2** in hand, we investigated its reduction to give bisNHC–aluminum(I) species. We found that $\text{K}_2\text{Fe}(\text{CO})_4$ can act as a suitable reducing agent for this purpose, whereas our attempts to reduce complex **2** with either KC_8 or sodium naphthalenide furnished only intractable product mixtures. Accordingly, the reduction of **2** with 1 molar equiv of $\text{K}_2\text{Fe}(\text{CO})_4$ was carried out in THF from -50°C to room temperature to afford $(\text{bisNHC})\text{Al}(\text{Br})[\text{Fe}(\text{CO})_4]$ (**3**), which could be isolated as colorless crystals in moderate yield (72%) (Scheme 2). Compound **3** is the first example of stable Al(I) complex bearing an NHC ligand.^{1b,18}

Scheme 2. Reduction of 2 with $\text{K}_2\text{Fe}(\text{CO})_4$ To Afford $[(\text{bisNHC})\text{Al}(\text{Br})[\text{Fe}(\text{CO})_4]]$ (3**)**



Compound **3** is soluble in THF and CH_2Cl_2 but exhibits low solubility in toluene and other aliphatic solvents. Because of the lower symmetry of complex **3** compared with **2**, four doublet resonance signals ($\delta = 0.95$, 1.01 , 1.22 , and 1.32 ppm) and two septet signals ($\delta = 2.50$ and 3.00 ppm) for the isopropyl groups are observed in the ^1H NMR spectrum in $\text{THF-}d_8$. In the infrared spectrum, the stretching frequencies for the carbonyl groups are observed at $\nu = 1982$, 1897 , 1859 , and 1819 cm^{-1} and are blue-shifted in comparison with those in $\text{Cp}^*\text{Al}[\text{Fe}(\text{CO})_4]$ ($\nu = 2024$, 1948 , 1903 cm^{-1} ; $\text{Cp}^* = \text{pentamethylcyclopentadienyl}$),¹⁹ suggesting a stronger electron-donating ability of the aluminum moiety in **3**. This is likely due to the strong σ -donating property of the bisNHC ligand. Figure 2 depicts the solid-state structure of complex **3**, which crystallizes in monoclinic space group $P2_1/c$. The Al center features a tetrahedral geometry, with coordination to two carbon centers of the bisNHC ligand and bromine and iron atoms. The iron center exhibits a trigonal-bipyramidal geometry with the bisNHC–Al moiety in an apical position. The Al–C bond distances [2.045(4) and 2.048(4) Å] are comparable to that in

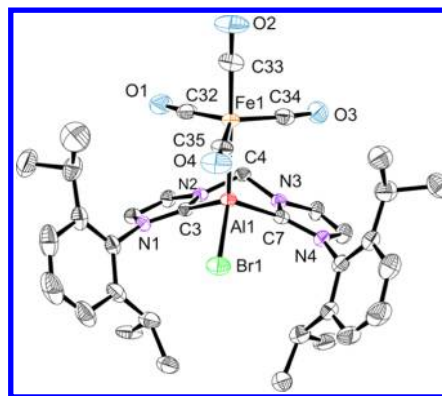
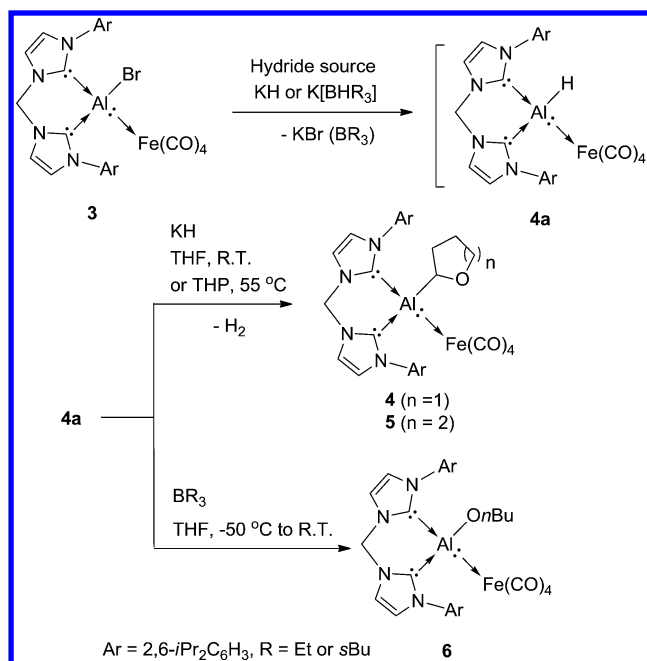


Figure 2. Molecular structure of **3**. Thermal ellipsoids are drawn at the 50% probability level. All of the hydrogen atoms and the solvent molecule have been omitted for clarity. Selected bond lengths (Å) and angles (deg): Al1–C3 2.045(4), Al1–C7 2.048(4), Al1–Br1 2.3173(11), Al1–Fe1 2.4062(11); C3–Al1–C7 88.73(14), C3–Al1–Br1 104.80(10), C7–Al1–Br1 103.84(11), C3–Al1–Fe1 112.57(10), C7–Al1–Fe1 113.54(11), Br1–Al1–Fe1 126.54(5).

$(\text{IPr})\text{AlI}_3$ [2.031(2) Å]^{16b} and slightly longer than those in the starting material **2** [2.018(5) and 2.027(5) Å]. The Al–Fe bond distance is longer than that in $\text{Cp}^*\text{Al–Fe}(\text{CO})_4$ [2.231(3) Å].¹⁹

After obtaining compound **3** as an Al(I) source, we targeted the synthesis of the corresponding hydridoaluminum(I) complex. Hence, potassium hydride (KH) was chosen first as a hydride source to react with **3** in THF at room temperature for 48 h (Scheme 3). However, the expected salt metathesis reaction did not lead to the desired Al(I)–H complex $(\text{bisNHC})\text{Al}(\text{H})[\text{Fe}(\text{CO})_4]$ (**4a**) but instead gave the complex $(\text{bisNHC})\text{Al}(2\text{-cyclo-OC}_4\text{H}_7)[\text{Fe}(\text{CO})_4]$ (**4**) bearing a THF moiety deprotonated at the α -carbon position attached to the aluminum center. A plausible explanation for the formation of **4** could be that the desired Al(I)–H complex **4a** is formed as an

Scheme 3. Activation of C–H and C–O Bonds Mediated by the Elusive Hydrido-Al(I)→Fe Complex 4a



elusive species (reactive intermediate) that metalates a THF molecule to yield compound **4** with concomitant elimination of dihydrogen. The formation of dihydrogen was additionally confirmed by ^1H NMR experiments: a resonance signal at $\delta = 4.53$ ppm corresponding to H_2 was observed from the reaction of **3** with KH at room temperature in $\text{THF-}d_8$ in a sealed NMR tube (see Figure 21s in the Supporting Information). The formation of H_2 instead of the anticipated HD can be explained by the degree of deuteration of $\text{THF-}d_8$ (99.5% D). In addition, the C–D bond is stronger than the C–H bond, that is, it is more favorable to deprotonate the C–H bond (isotope effect). Moreover, the detailed mechanism was further elucidated by DFT calculations (*vide infra*).

The composition of complex **4** was determined by a combination of NMR spectroscopic and X-ray crystallographic studies. The molecular structure of **4** is portrayed in Figure 3.

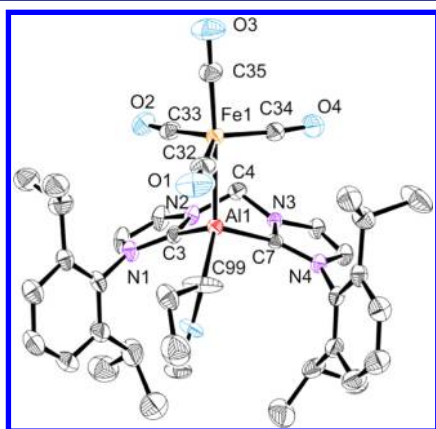


Figure 3. Molecular structure of **4**. Thermal ellipsoids are drawn at the 50% probability level. All of the hydrogen atoms have been omitted for clarity. Selected bond lengths (Å) and angles (deg): Al1–C3 2.060(5), Al1–C7 2.059(4), Al1–Fe1 2.4834(14), Al1–C99 1.998(5); C99–Al1–C7 110.2(2), C99–Al1–C3 110.3(2), C7–Al1–C3 87.48(17), C99–Al1–Fe1 124.29(15), C7–Al1–Fe1 109.68(12), C3–Al1–Fe1 108.68(13).

The THF moiety is metalated by the Al(I) center at the α -carbon position and stays intact at ambient temperature without any ring opening and/or bond cleavage. This is remarkable since conventional α -metalation of THF with organolithium and organopotassium reagents normally initiates ring opening and cleavage of C–O and C–C bonds to form ethylene and the enolate of acetaldehyde at ambient temperature.²⁰ Very recently, Mulvey and co-workers developed a methodology based on the bimetallic bases $[(\text{TMEDA})\text{Na}(\mu\text{-TMP})(\mu\text{-CH}_2\text{SiMe}_3)\text{Zn}(\text{CH}_2\text{SiMe}_3)]$ (TMP = 2,2,6,6-tetramethylpiperidine) and $[(\text{THF})\text{Li}(\text{TMP})(\text{TMP})\text{Al}(\text{iBu})_2]$ for α -metalation of cyclic ethers and analogues, in which the cyclic ether anions are cooperatively stabilized by the Na/Zn²¹ and Li/Al²² cations, respectively. In contrast to the reported bimetallic systems, in complex **4** the THF anion is stabilized only by the Al center. Moreover, in the bimetallic base systems, alkaline bases are crucial for the activation of inert C–H bonds, since the organozinc or -aluminum reagents alone are not basic enough to deprotonate cyclic ethers and analogues. It is also noteworthy that a recent report by Mulvey and co-workers showed that the α -metalation of THF with the bimetallic base $\text{LiTMP}\cdot\text{Al}(\text{iBu})_3$ is a two-step process involving initial metalation of THF with LiTMP followed by trapping of the metalated species by the Al reagent.²³ In contrast, we did not observe any reaction between KH and THF, indicating that the α -metalation of THF occurs through hydrido-Al(I) complex **4a** directly.

As a result of the substitution of one hydrogen atom at the α -C position of THF with an Al atom, the α -C atom is bonded to four different atoms (Al, O, C, and H), rendering it chiral. The consequence of this induced chirality is the complete loss of symmetry of compound **4** compared with the starting materials **2** and **3**. Thus, all eight methyl groups in the isopropyl moieties are inequivalent, and eight doublet resonance signals ($\delta = 0.95, 0.97, 0.98, 1.04, 1.09, 1.13, 1.30, \text{ and } 1.31$ ppm) were observed in the ^1H NMR spectrum in $\text{THF-}d_8$ solution. Moreover, two ^{13}C resonance signals for the NCN moiety were found in the ^{13}C NMR spectrum ($\delta = 177.0$ and 177.4 ppm). The ^{13}C NMR chemical shifts for the AlCHO and OCH_2 subunits were

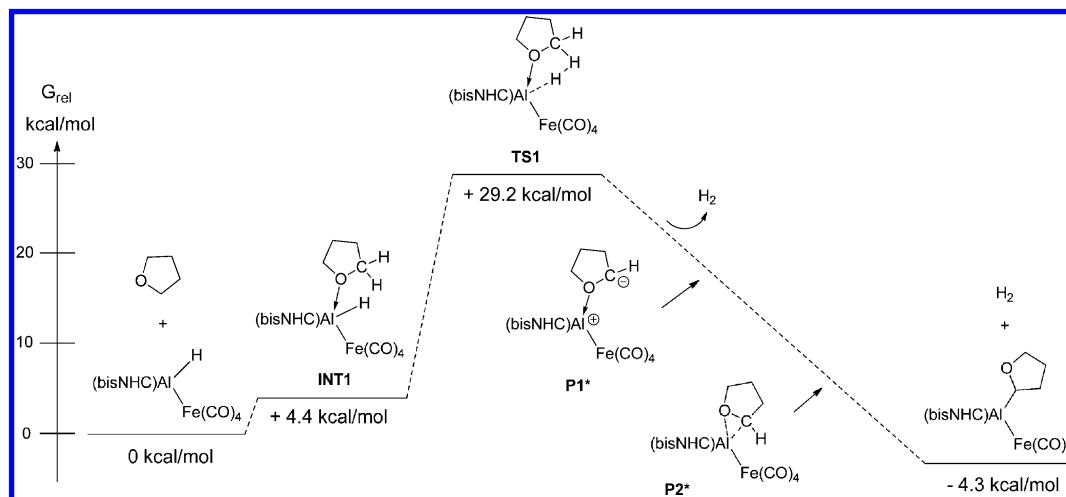


Figure 4. Reaction mechanism for the formation of **4** and H_2 starting from **4a** and THF, derived from DFT calculations at the B97-D/def2-TZVP(THF)//B97-D/6-31G*[Al,Fe def2-TZVP] level of theory. *The determination of **P1** and **P2** is somewhat complicated. Both are not intermediates in the sense that tight optimization does not yield these structures. However, we include them in the energy profile since after the elimination of H_2 , species **P1** remains and then isomerizes to **P2**.

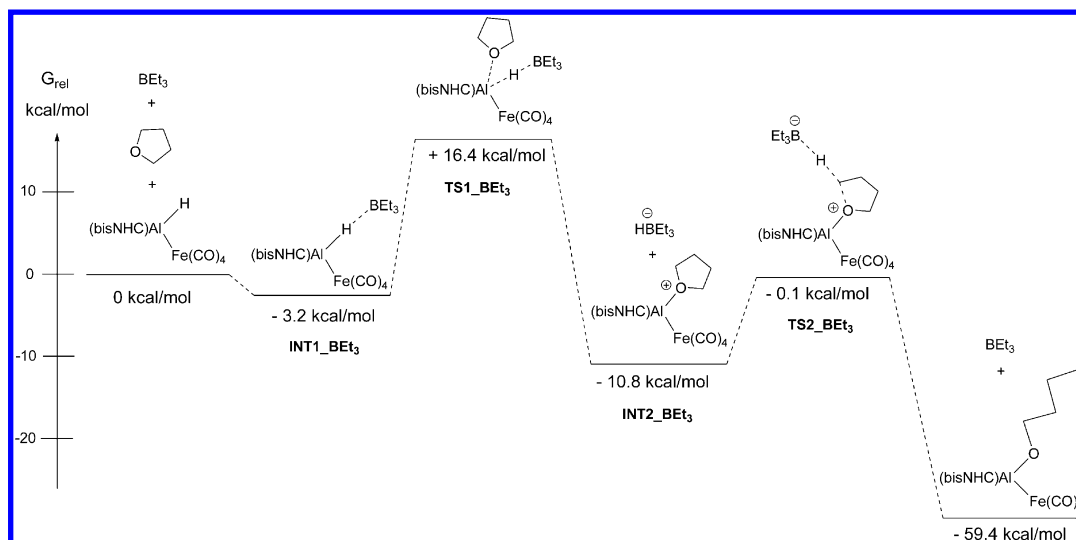


Figure 5. Mechanism for the formation of **6** derived from DFT calculations at the B97-D/def2-TZVP(THF)//B97-D/6-31G*[Al,Fe def2-TZVP] level of theory.

observed at $\delta = 69.1$ and 74.7 ppm (broad as a result of coupling with the quadrupolar ^{27}Al nucleus), respectively.

Prompted by the facile α -metalation of THF with the elusive $\text{Al(I)}\text{--H}$ complex **4a**, we further explored the α -metalation of THP, the six-membered-ring homologue of THF. In close analogy, THP was also readily α -metalated to yield $(\text{bisNHC})\text{--Al(2-cyclo-C}_3\text{H}_9\text{O)[Fe(CO)}_4\text{]}$ (**5**) as the sole product when **3** was reacted with an excess amount (2 molar equiv) of KH in THP at 55°C for 48 h (Scheme 3). Because of the chirality of the THP carbon attached to the Al(I) center, complex **5** exhibits features similar to those of **4** for the protons as well as the ^{13}C nuclei at the ligand in the ^1H and ^{13}C NMR spectra in $\text{THF-}d_8$, respectively (see Figures 9s–11s in the Supporting Information). For instance, the protons of the methine groups are observed as four septets ($\delta = 2.10, 2.26, 3.28$, and 3.61 ppm) in the ^1H NMR spectrum in $\text{THF-}d_8$, and two resonance signals for the carbene carbon (NCN) nuclei ($\delta = 177.1$ and 177.3 ppm) could be observed in the ^{13}C NMR spectrum. In the high-resolution mass spectrum, the signal of the molecular peak could not be observed, whereas the molecular fragment corresponding to loss of the THP moiety and one CO was revealed at m/z 637.2475 (calcd m/z 637.2416). The latter result shows that **4a** is also capable of α -metalation of THP, and it represents the first example in which a low-valent main-group hydrido complex activates the relatively inert C–H bond of cyclic ethers, hitherto the domain of transition-metal complexes.²⁴

In order to better understand the mechanism for the α -C–H activation of THF with **4a** to form **4**, we carried out DFT calculations at the B97-D/def2-TZVP(THF)//B97-D/6-31G*-[Al,Fe def2-TZVP] level of theory (Figure 4). The calculations revealed that the first step is the coordination of the THF molecule to the Al center in **4a** to afford the intermediate **INT1** with a five-coordinate aluminum center, which is succeeded by the H–H interaction of the Al–H and C–H moieties to form the five-membered-ring transition state **TS1** with an associated free energy of $+29.2$ kcal mol $^{-1}$. **TS1** is rather high considering the reaction conditions. However, when the margin of error associated with DFT methods is taken into account, this mechanism is still viable. **TS1** is followed by the H_2 elimination step, also observed experimentally (vide supra), to generate the

zwitterionic species **P1**, which immediately rearranges, without activation barrier, to afford the product (-4.3 kcal mol $^{-1}$).

Interestingly, when $\text{K[BHR}_3\text{]}$ ($\text{R} = \text{Et}, \text{sBu}$) as opposed to KH was used as the hydride source to react with **3** in THF at room temperature, the reaction afforded the THF-ring-opened complex $(\text{bisNHC})\text{Al(OnBu)[Fe(CO)}_4\text{]}$ (**6**) as the product in 62% yield (Scheme 3). The OnBu group in the product originates from C–O bond cleavage of a THF solvent molecule, since when the reaction was carried out in $\text{THF-}d_8$, all of the proton signals corresponding to the OnBu moiety vanished when compared with the ^1H NMR spectrum of **6** in $\text{THF-}d_8$ (see Figure 15s in the Supporting Information). The composition of **6** was determined by NMR spectroscopy, elemental analysis, and IR spectroscopy. Unfortunately, numerous attempts to crystallize complex **6** under various conditions were unsuccessful. The proton signals for the OnBu group were observed at $\delta = 0.49\text{--}0.55$ ppm as a multiplet (7H) and $\delta = 2.74$ ppm as a triplet (2H) in the ^1H NMR spectrum in $\text{THF-}d_8$. The corresponding ^{13}C chemical shifts could be obtained at $\delta = 14.7, 19.4, 37.3$, and 61.6 ppm in the ^{13}C NMR spectrum (see Figures 12s–14s in the Supporting Information). Related C–O bond cleavage of THF to form ring-opened products has also been observed with transition-metal hydrido complexes²⁵ and a “frustrated Lewis pair” (FLP).²⁶ DFT calculations suggested that the $\text{Al(I)}\text{--H}$ bond in **4a** is activated by the Lewis acid BEt_3 (formed in situ from $\text{K[BHEt}_3\text{]}_2$) through an FLP-like interaction to afford **INT1_BEt3** (Figure 5). The interaction of the Al center with the THF molecule further weakens the Al–H bond, leading to transition state **TS1_BEt3** ($+16.4$ kcal mol $^{-1}$) and the rate-determining barrier for the overall reaction ($+19.6$ kcal mol $^{-1}$), which prompts the Al–H bond dissociation to form **INT2_BEt3** (-10.8 kcal mol $^{-1}$). Subsequent hydride transfer from the HBEt_3^- anion to the THF moiety triggers the C–O bond cleavage, leading to the highly stable product **6** (-59.4 kcal/mol).

In order to generate an isolable monovalent group 13 metal hydrido analogue of **4a**, we shifted our focus to the synthesis of the hydrido-Ga(I) \rightarrow Fe complex **9**. Because of the higher electronegativity of gallium versus aluminum, we envisaged that the Ga–H bond should exhibit greater covalent character than the corresponding Al–H bond, implying a higher stability of

Scheme 4. Syntheses of Complexes 7–9

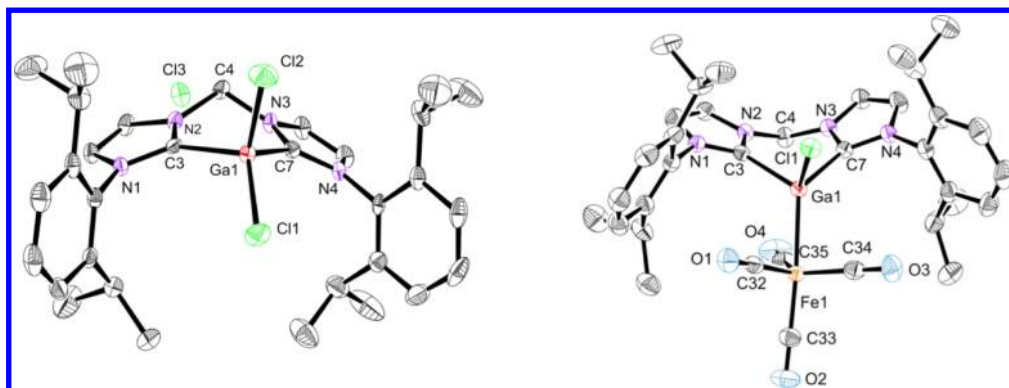
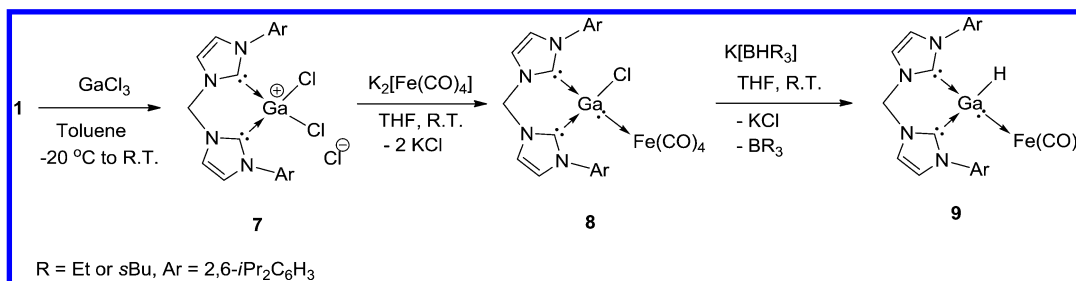


Figure 6. Molecular structures of (left) **7** and (right) **8**. Thermal ellipsoids are drawn at the 50% probability level. All of the hydrogen atoms have been omitted for clarity. Selected bond lengths (Å) and angles (deg) for **7**: Ga1–C3 2.000(4), Ga1–C7 2.006(3), Ga1–Cl1 2.1431(10), Ga1–Cl2 2.1584(10); C3–Ga1–C7 93.61(15), C3–Ga1–Cl1 114.63(10), C7–Ga1–Cl1 115.20(11), C3–Ga1–Cl2 109.25(10), C7–Ga1–Cl2 109.52(10), Cl1–Ga1–Cl2 113.00(5). For **8**: Ga1–C3 2.0827(18), Ga1–C7 2.0829(18), Ga1–Cl1 2.2463(5), Ga1–Fe1 2.3539(4); C3–Ga1–C7 89.94(7), C3–Ga1–Cl1 102.30(5), C7–Ga1–Cl1 97.38(5), C3–Ga1–Fe1 119.27(5), C7–Ga1–Fe1 126.10(5), Cl1–Ga1–Fe1 116.349(16).

complex **9** versus **4a**. In fact, the isolable complex **9** was expected to be formed through a similar synthetic protocol as applied for the synthesis of the elusive complex **4a**. Accordingly, we synthesized the starting material [(bisNHC)GaCl₂]⁺Cl[−] (**7**) by the reaction of **1** with 1 molar equiv of GaCl₃ in toluene at room temperature (Scheme 4), and **7** was isolated as an off-white solid in 90% yield. The precursor **7** was readily reduced by K₂[Fe(CO)₄] in THF at ambient temperature to afford the first bisNHC-stabilized Ga^ICl complex, (bisNHC)Ga(Cl)[Fe(CO)₄] (**8**).²⁷ The compositions of **7** and **8** were elucidated by single-crystal X-ray diffraction analyses, elemental analyses, and IR spectroscopy as well as ¹H and ¹³C NMR spectroscopy for **7**. Compound **8** is extremely insoluble in organic solvents, preventing its characterization by solution NMR spectroscopy.

Complex **7** has a solubility similar to that seen with complex **2**. The ¹H NMR spectrum indicates a high symmetry of **7** in CD₂Cl₂ solution. For instance, the protons of the isopropyl groups are revealed as two doublet resonance signals (δ = 1.06 and 1.17 ppm) for the methyl groups and one septet (δ = 2.35 ppm) for the methine moieties. The crystal structure analyses of compounds **7** and **8** are depicted in Figure 6. The structure motifs of **7** and **8** are similar to those of **2** and **3**, respectively. In compound **7**, the Ga atom has a tetrahedral configuration, and the Ga–C bond distances of 2.000(4) and 2.006(3) Å are close to those in mono-NHC-stabilized Ga(III) complexes.²⁸ The Ga atom in **8** is tetrahedrally coordinated with two carbon atoms and one chloride atom along with a Fe(CO)₄ moiety; this is similar to the situation observed for Ga(I) complexes stabilized by neutral bidentate nitrogen-containing ligands.^{7,29}

The chloride/hydride exchange of **8** with 1 molar equiv of K[BHR₃] (R = Et, sBu) as a hydride source in THF at room temperature indeed afforded the isolable hydrido-Ga(I)→Fe

complex (bisNHC)Ga(H)[Fe(CO)₄] (**9**), which is stabilized by the bisNHC ligand **1** and a Fe(CO)₄ moiety (Scheme 4). Remarkably, compound **9** does not react with THF and THP. It was characterized by NMR and IR spectroscopy, elemental analysis, and single-crystal X-ray diffraction. It has a relatively low solubility in THF and is also marginally soluble in toluene and *n*-hexane. The proton signal for Ga–H is revealed at δ = 4.58 ppm in the ¹H NMR spectrum in THF-*d*₈, which is comparable to those of LGaH₂ [L = CH(CMeNAr)₂, Ar = 2,6-*i*Pr₂C₆H₃] (δ = 4.53 ppm)³⁰ and (TMEDA)Ga(H)[Cr(CO)₅] (δ = 5.03 ppm).⁷ Single crystals suitable for X-ray diffraction analysis were obtained from a saturated solution in THF at 0 °C, and the structure is portrayed in Figure 7. Complex **9** crystallizes in the monoclinic space group *P*2₁/*c*, where the Ga center is tetrahedrally coordinated by the C3, C7, Fe1, and H3 atoms. The Ga1–Fe1 bond distance is slightly longer than that in the starting material (bisNHC)Ga(Cl)[Fe(CO)₄] **8**. This is in accordance with the observation for silylene–metal complexes that the Si–M bond is longer when there is an electron-donating group attached to the silicon center.^{2a,31}

To obtain a rational understanding for the formation and stability of the hydrido-Ga(I) complex **9**, which is inert toward THF, in contrast to its aluminum analogue **4a**, we carried out DFT calculations probing the hypothetical C–O bond activation of THF with **9** (Figure 8). The overall reaction to form the C–O bond cleavage product (bisNHC)Ga(OnBu)[Fe(CO)₄] is indeed thermodynamically favorable, with an exergonicity of −27.7 kcal mol^{−1} with respect to the starting materials [it should be noted that this is less exergonic by 31.7 kcal mol^{−1} compared with the case of the aluminum analogue (*vide supra*)]. However, the free energy of activation for the rate-determining step (+34.3 kcal mol^{−1}) is very high compared

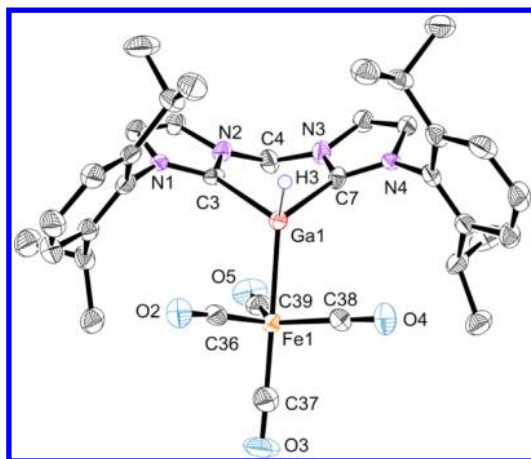


Figure 7. Molecular structure of **9**. Thermal ellipsoids are drawn at the 50% probability level; all of the hydrogen atoms except Ga–H have been omitted for clarity. Selected bond lengths (Å) and angles (deg): Ga1–C3 2.084(5), Ga1–C7 2.093(6), Ga1–Fe1 2.4010(12), Ga1–H3 1.84(6); C3–Ga1–C7 88.3(2), C3–Ga1–Fe1 116.72(16), C7–Ga1–Fe1 121.41(16), C3–Ga1–H3 103(2), C7–Ga1–H3 103(2), Fe1–Ga1–H3 119(2).

with that for the aluminum complex (only +19.6 kcal mol^{−1}), suggesting notably higher kinetic stability of **9** toward THF activation. These findings hence rationalize the inertness of **9** with respect to C–O bond activation of cyclic ethers, in accordance with our experimental findings. We also investigated the possible C–H bond activation process analogous to the observed reaction of **4a** (Figure 9) and found that the

activation barrier **TS1_Ga** is extremely high (+84.2 kcal mol^{−1}) and that the product is less stable than the reactants (+47.5 kcal mol^{−1}). Therefore, this reaction cannot proceed, again in accordance with our experimental findings.

SUMMARY AND CONCLUSION

We have investigated the synthesis of the first hydrido-Al(I):→Fe and hydrido-Ga(I):→Fe complexes **4a** and **9**, respectively, employing the chelating bisNHC ligand **1**. These complexes result from stepwise redox transformations of the corresponding [(bisNHC)M^{III}X₂]⁺X[−] complexes **2** (M = Al, X = Br) and **7** (M = Ga, X = Cl) with K₂Fe(CO)₄ and subsequent halogen/hydride exchange reactions with KH and K[BHR₃] in THF and THP solutions, respectively. Remarkably, while (bisNHC)Al(H)[Fe(CO)₄] (**4a**) is an elusive species that reacts readily with THF and THP under C–H or C–O activation, its Ga analogue **9** is inert in ethereal solvents and could be isolated and structurally characterized. The nature of the cleavage product formed from THF or THP depends on the hydride source used to prepare **4a** in THF or THP starting from the Al(I) precursor (bisNHC)Al(Br)[Fe(CO)₄] (**3**). When KH was allowed to react with **3** in THF and THP, (bisNHC)Al(2-*cyclo*-OC₄H₇)[Fe(CO)₄] (**4**) and (bisNHC)Al(2-*cyclo*-OC₅H₉)[Fe(CO)₄] (**5**) were formed via α-C–H bond activation of THF and THP, respectively, and could be isolated in good yields. In both complexes **4** and **5**, the cyclic ether anions stay intact at room temperature without any ring opening and bond cleavage. In contrast, the metathesis reaction of **3** with K[BHR₃] (R = Et, *s*Bu) led to the formation of the ring-opening product (bisNHC)Al(OnBu)[Fe(CO)₄] (**6**) with the activation of a

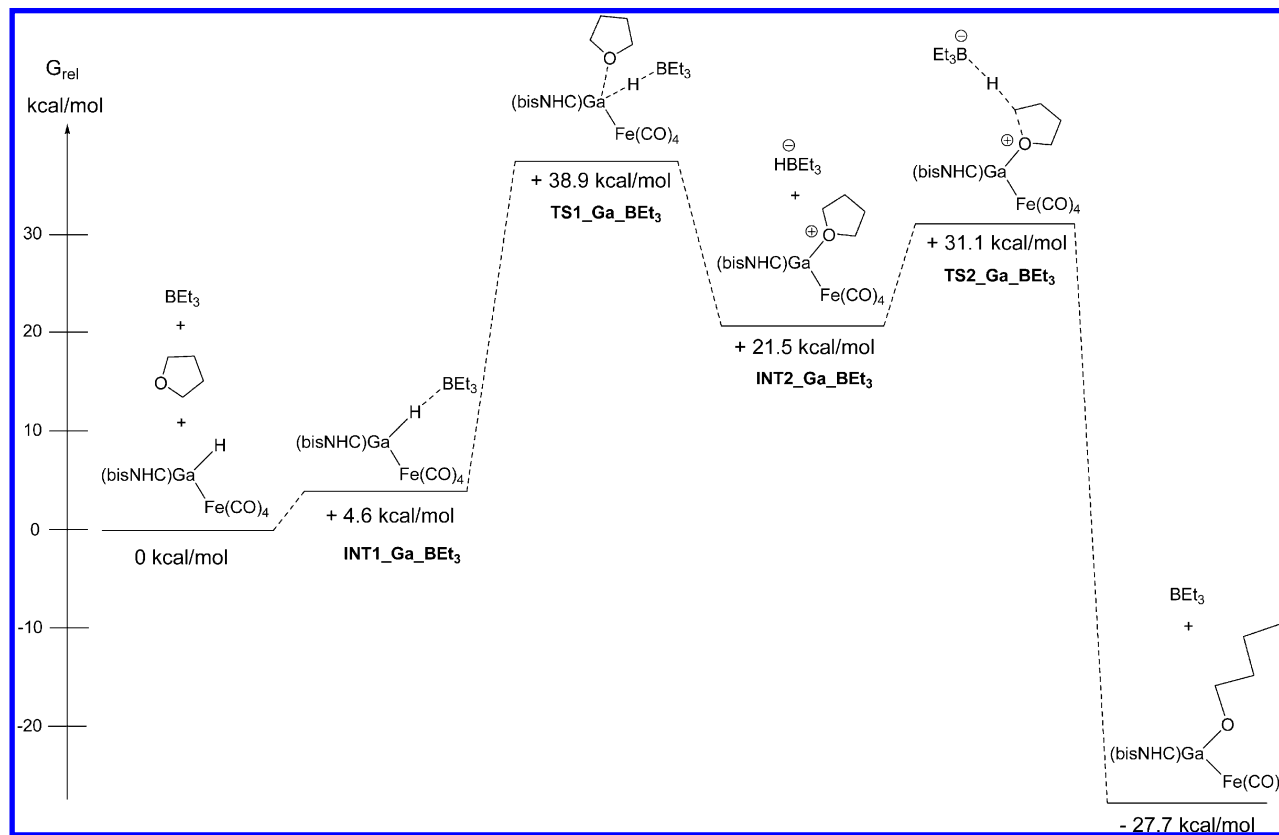


Figure 8. Mechanism for the hypothetical C–O bond cleavage of THF with **9** derived from DFT calculations at the B97-D/def2-TZVP(THF)//B97-D/6-31G*[Ga,Fe def2-TZVP] level of theory.

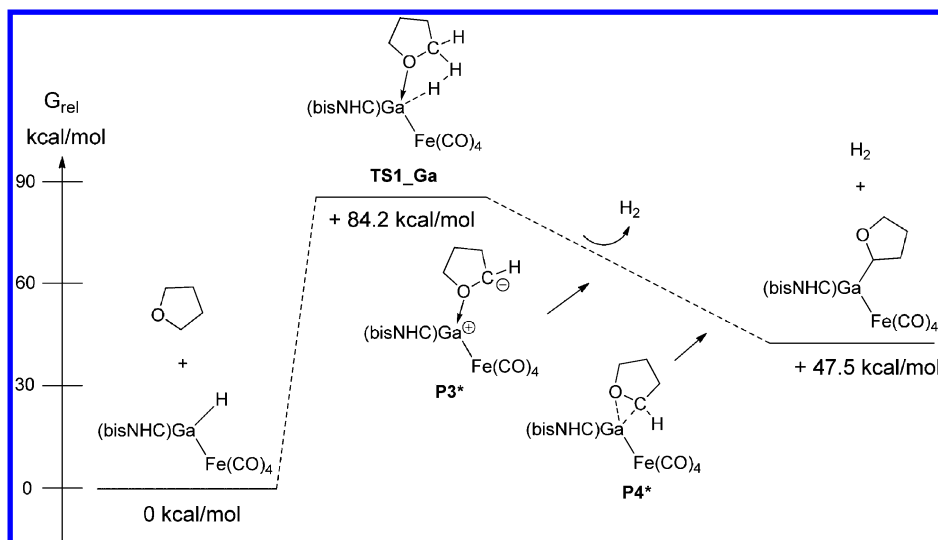


Figure 9. Mechanism for the hypothetical C–H bond cleavage of THF with **9** derived from DFT calculations at the B97-D/def2-TZVP(THF)//B97-D/6-31G*[Ga,Fe def2-TZVP] level of theory. *The determination of **P3** and **P4** is somewhat complicated. Both are not intermediates in the sense that tight optimization does not yield these structures. However, we include them in the energy profile since after the elimination of H₂, species **P3** remains and then isomerizes to **P4**.

C–O bond of THF. The detailed mechanisms for C–H and C–O bond activation mediated by **4a** were elucidated by DFT calculations. The C–O bond activation is assisted by the Lewis acid BR₃ (R = Et, *s*Bu) generated in situ from K[BHR₃] after the Br/H ligand exchange reaction with **3**. The inert nature of the Ga analogue **9** with respect to hypothetical C–O bond activation of THF was rationalized by DFT calculations, where a substantial kinetic barrier was found despite the fact that the overall process is exergonic. The unexpectedly high reactivity of Al(I) hydrido complex **4a** opens new doorways to facile and selective C–H metalation reactions of functionalized hydrocarbons with aluminum. The suitability of elusive **4a** and its isolable Ga analogue **9** to act as selective metalation reagents for other functionalized organic substrates is currently under investigation.

EXPERIMENTAL SECTION

General Procedures. All of the experiments were carried out under dry oxygen-free nitrogen using standard Schlenk techniques. Solvents were dried by standard methods and freshly distilled and degassed prior to use. The NMR spectra were recorded on Bruker spectrometers (AV400 or AV200) referenced to residual solvent signals as internal standards (¹H NMR: CD₂Cl₂ at 5.32 ppm, THF-*d*₈ at 1.72 and 3.58 ppm; ¹³C{¹H} NMR: CD₂Cl₂ at 53.8 ppm, THF-*d*₈ at 25.3 and 67.2 ppm). Abbreviations: s = singlet; m = multiplet; br = broad, quint = quintet, sept = septet. Unambiguous signal assignments were made by employing a combination of 2D H,C heteronuclear multiple-quantum correlation (HMQC) and distortionless enhancement by polarization transfer (DEPT) NMR experiments. Concentrated solutions of samples in CD₂Cl₂ or THF-*d*₈ were sealed off in an NMR tube under vacuum for measurements. Melting points were recorded on a Melting Point Tester device (BSGT Company) and are uncorrected. Each sample was sealed off in capillary under vacuum and measured in duplicate. Mass spectra were recorded on an Orbitrap LTQ XL mass spectrometer (Thermo Scientific), and the raw data were evaluated using the Xcalibur computer program. For the single-crystal X-ray structure analyses, each crystal was mounted on a glass capillary in perfluorinated oil and measured in a cold N₂ flow. The data for all compounds were collected on an Oxford Diffraction Supernova, single source at offset, atlas at 150 K (Cu Kα radiation, λ = 1.5418 Å) or an Agilent Technologies Xcalibur S Sapphire at 150 K (Mo Kα radiation, λ = 0.71073 Å). The structures were solved by direct

methods and refined on F² with the SHELX-97 software package.³² The positions of the H atoms were calculated and considered isotropically according to a riding model. The H atom of Ga–H in complex **9** was positioned from difference Fourier maps and refined freely. The starting material bisNHC **1**^{3a} and K₂Fe(CO)₄³³ were synthesized according to the published procedures. The other commercially available materials were used as received.

[(bisNHC)AlBr₂]⁺Br[−] (2**).** The bisNHC ligand (**1**) (2.49 g, 5.3 mmol) and anhydrous AlBr₃ (1.33 g, 5 mmol) were placed in a Schlenk flask (250 mL) in the glovebox. Toluene (80 mL) was transferred to the flask via cannula under vigorous stirring at −78 °C. The formed brown suspension was allowed to warm to room temperature and stirred for another 12 h. The off-white product was collected by filtration, washed with *n*-hexane (10 mL) twice, and dried in vacuo for 12 h. Yield: 3.38 g, 4.6 mmol (92%). Mp: 209 °C. A crystal suitable for X-ray diffraction analysis was obtained by recrystallization in CH₂Cl₂/*n*-hexane at −30 °C. ¹H NMR (200.1 MHz, CD₂Cl₂, 298 K, ppm): δ = 1.05 (d, 12H, CH(CH₃)₂, ³J_{H,H} = 6.8 Hz), 1.18 (d, 12H, CH(CH₃)₂, ³J_{H,H} = 6.8 Hz), 2.36 (sept, 4H, CH(CH₃)₂, ³J_{H,H} = 6.8 Hz), 7.22 (d, 2H, CH=CH, ³J_{H,H} = 1.6 Hz), 7.27 (d, 4H, Ar-H, ³J_{H,H} = 7.6 Hz), 7.51 (t, 2H, Ar-H, ³J_{H,H} = 7.6 Hz), 7.83 (s, 2H, NCH₂N), 8.85 (d, 2H, CH=CH, ³J_{H,H} = 1.6 Hz). ¹³C{¹H} NMR (50.2 MHz, CD₂Cl₂, 298 K, ppm): δ = 23.0, 26.0 (CH(CH₃)₂), 28.8 (CH(CH₃)₂), 59.9 (NCH₂N), 124.6 (CH=CH), 125.2, 125.5 (Ar-CH), 128.5, 129.3 (Ar-C), 131.7 (Ar-CH), 132.6, 145.7 (Ar-C). The ¹³C resonance signal for NCN was not observed. Anal. Calcd for C₃₁H₄₀AlBr₂N₄·1/2(*n*-hexane): C, 52.46; N, 7.20; H, 6.09. Found: C, 52.33; N, 7.25; H, 5.83.

(bisNHC)Al(Br)[Fe(CO)₄] (3**).** Compound **2** (0.37 g, 0.5 mmol) and K₂Fe(CO)₄ (0.11 g, 0.5 mmol) were placed in a Schlenk flask (100 mL) in the glovebox. THF (60 mL) was transferred to the flask via cannula under stirring at −78 °C, and a slightly yellow suspension was formed. The mixture was allowed to warm to room temperature, stirred for another 5 h, and filtered to remove the inorganic precipitate. The obtained light-yellow filtrate was concentrated to ca. 5 mL and left at 0 °C for 12 h to afford compound **3** as a colorless crystalline solid. Yield: 0.27 g, 0.36 mmol (72%). Mp: 283 °C (dec.). ¹H NMR (200.1 MHz, THF-*d*₈, 298 K, ppm): δ = 0.95 (d, 6H, CH(CH₃)₂, ³J_{H,H} = 6.8 Hz), 1.01 (d, 6H, CH(CH₃)₂, ³J_{H,H} = 6.6 Hz), 1.22 (d, 6H, CH(CH₃)₂, ³J_{H,H} = 6.8 Hz), 1.32 (d, 6H, CH(CH₃)₂, ³J_{H,H} = 6.6 Hz), 2.50 (sept, 2H, CH(CH₃)₂, ³J_{H,H} = 6.8 Hz), 3.00 (sept, 2H, CH(CH₃)₂, ³J_{H,H} = 6.6 Hz), 6.65 (s, 2H, NCH₂N), 7.15–7.34 (m, 6H, Ar-H), 7.39 (d, 2H, CH=CH, ³J_{H,H} = 1.6 Hz), 7.75 (d, 2H, CH=CH, ³J_{H,H} = 1.6 Hz). ¹³C{¹H} NMR (100.2 MHz, THF-*d*₈, 298

K, ppm): δ = 22.3, 22.5, 25.4, 25.6 (CH(CH₃)₂), 27.8, 28.2 (CH(CH₃)₂), 60.9 (NCH₂N), 121.3 (CH=CH), 123.7, 124.0 (Ar-CH), 125.9 (CH=CH), 130.2 (Ar-CH), 134.6 (Ar-C), 145.6, 145.9 (Ar-CN), 170.1 (NCN), 219.2 (CO). IR (KBr, cm⁻¹): ν = 1982, 1897, 1859, 1819 (CO). Anal. Calcd for C₃₅H₄₀AlBrFeN₄O₄·THF: C, 57.44; N, 6.87; H, 5.93. Found: C, 57.42; N, 7.19; H, 5.60.

(bisNHC)Al(2-cyclo-OC₄H₇)[Fe(CO)₄] (4). Compound 3 (74 mg, 0.1 mmol) and KH (12 mg, 0.3 mmol) were placed in a Schlenk flask (50 mL). THF (20 mL) was transferred to the flask via cannula at room temperature. The mixture was stirred for 48 h and then filtered, and the filtrate was concentrated to ca. 3 mL and left at -30 °C for 24 h to give compound 4 as a colorless crystalline solid. The product was collected by decantation of the supernatant and dried in vacuo for several hours. Yield: 50 mg, 0.068 mmol (68%). Mp: 258 °C (dec.). ¹H NMR (400.2 MHz, THF-*d*₈, 298 K, ppm): δ = 0.47 (m, 1H, CH₂ in cyclo-C₄H₇O), 0.76 (m, 1H, CH₂ in cyclo-C₄H₇O), 0.95 (d, 3H, CH(CH₃)₂, ³J_{H,H} = 6.8 Hz), 0.97 (d, 3H, CH(CH₃)₂, ³J_{H,H} = 6.8 Hz), 0.98 (d, 3H, CH(CH₃)₂, ³J_{H,H} = 6.8 Hz), 1.04 (d, 3H, CH(CH₃)₂, ³J_{H,H} = 6.8 Hz), 1.09 (d, 3H, CH(CH₃)₂, ³J_{H,H} = 6.4 Hz), 1.13 (d, 3H, CH(CH₃)₂, ³J_{H,H} = 6.8 Hz), 1.30 (d, 3H, CH(CH₃)₂, ³J_{H,H} = 6.8 Hz), 1.31 (d, 3H, CH(CH₃)₂, ³J_{H,H} = 6.4 Hz), 1.52 (m, 1H, CH₂ in cyclo-C₄H₇O), 2.05–2.21 (m, 4H, CH₂ in cyclo-C₄H₇O (1H) + Al-CHO (1H) + CH(CH₃)₂ (2H)), 3.09 (m, 1H, CH₂ in cyclo-C₄H₇O), 3.41 (sept, 1H, CH(CH₃)₂, ³J_{H,H} = 6.8 Hz), 3.50 (sept, 1H, CH(CH₃)₂, ³J_{H,H} = 6.8 Hz), 6.64 (d, 1H, NCH₂N, ²J_{H,H} = 13.2 Hz), 6.74 (d, 1H, NCH₂N, ²J_{H,H} = 13.2 Hz), 7.13–7.35 (m, 6H, Ar-CH), 7.36 (d, 1H, CH=CH, ³J_{H,H} = 1.6 Hz), 7.38 (d, 1H, CH=CH, ³J_{H,H} = 1.6 Hz), 7.72 (d, 1H, CH=CH, ³J_{H,H} = 1.6 Hz), 7.73 (d, 1H, CH=CH, ³J_{H,H} = 1.6 Hz). ¹³C{¹H} NMR (100.2 MHz, THF-*d*₈, 298 K, ppm): δ = 22.8, 23.3, 23.6, 23.7, 25.9, 26.1, 26.2, 26.4, 26.5, 26.7 (CH(CH₃)₂ and CH₂ in cyclo-OC₄H₇), 28.4, 28.6, 29.3 (CH(CH₃)₂), 62.0 (NCH₂N), 69.1 (OCH₂), 74.7 (br, Al-CHO), 122.2, 122.7 (CH=CH), 124.1, 124.2, 124.5, 125.0 (Ar-CH), 126.3, 126.4 (CH=CH), 130.6, 130.7 (Ar-CH), 136.1, 136.4 (Ar-C), 146.8, 146.9, 147.0, 147.2 (Ar-CN), 177.0, 177.4 (NCN), 222.0 (CO). IR (KBr, cm⁻¹): ν = 2739 (AlC-H), 1966, 1860, 1850 (CO). Anal. Calcd for C₃₉H₄₇AlFeN₄O₅: C, 63.76; N, 7.63; H, 6.45. Found: C, 63.09; N, 6.96; H, 6.82.

(bisNHC)Al(2-cyclo-OC₅H₉)[Fe(CO)₄] (5). Compound 3 (74 mg, 0.1 mmol) and KH (12 mg, 0.3 mmol) were placed in a Schlenk flask (50 mL). THP (20 mL) was transferred to the flask via cannula at room temperature. The mixture was stirred for 48 h at 55 °C, and then all of the volatiles were removed under reduced pressure. The residue was extracted with THF (20 mL) and filtered to obtain a brown solution. The solution was concentrated to ca. 10 mL and left at -30 °C for 24 h to give compound 5 as a colorless precipitate. The product was collected by decantation of the supernatant and dried in vacuo for several hours. Unfortunately, attempts to obtain a single crystal of 5 suitable for X-ray diffraction analysis were unsuccessful. Yield: 52 mg, 0.070 mmol (70%). Mp: 252 °C (dec.). ¹H NMR (400.2 MHz, THF-*d*₈, 298 K, ppm): δ = 0.23 (m, 1H, CH₂ in cyclo-OC₅H₉), 0.76–0.93 (m, 2H, CH₂ in cyclo-OC₅H₉), 0.94 (d, 3H, CH(CH₃)₂, ³J_{H,H} = 6.8 Hz), 0.99 (d, 6H, CH(CH₃)₂, ³J_{H,H} = 6.8 Hz), 1.07 (d, 6H, CH(CH₃)₂, ³J_{H,H} = 6.8 Hz), 1.17 (d, 3H, CH(CH₃)₂, ³J_{H,H} = 6.8 Hz), 1.29 (d, 3H, CH(CH₃)₂, ³J_{H,H} = 6.8 Hz), 1.37 (d, 3H, CH(CH₃)₂, ³J_{H,H} = 6.8 Hz), 1.05–1.25 (m, 4H, CH₂ in cyclo-OC₅H₉), 1.97 (m, 1H, OCH₂), 2.10 (sept, 1H, CH(CH₃)₂, ³J_{H,H} = 6.8 Hz), 2.26 (m, 1H, CH(CH₃)₂, 2.62 (m, 1H, Al-CHO), 3.02 (m, 1H, OCH₂), 3.28 (sept, 1H, CH(CH₃)₂, ³J_{H,H} = 6.8 Hz), 3.61 (m, 1H, CH(CH₃)₂), 6.64 (d, 1H, NCH₂N, ²J_{H,H} = 12.8 Hz), 6.67 (d, 1H, NCH₂N, ²J_{H,H} = 12.8 Hz), 7.15–7.43 (m, 8H, Ar-H (6H) + CH=CH (2H)), 7.71 (d, 1H, CH=CH, ²J_{H,H} = 1.6 Hz). ¹³C{¹H} NMR (100.2 MHz, THF-*d*₈, 298 K, ppm): δ = 22.6, 23.6, 23.7, 24.0, 25.6, 26.1, 26.4, 26.5, (CH(CH₃)₂), 27.3, 28.1, 28.7 (CH₂ in cyclo-OC₅H₉), 28.3, 28.8, 29.2, 29.3 (CH(CH₃)₂), 61.8 (NCH₂N), 71.0 (OCH₂ in cyclo-OC₅H₉), ca. 75.0 (OCH in cyclo-OC₅H₉; not observed in the ¹³C NMR spectrum, but it can be assigned from the ¹H,¹³C-HMQC NMR spectrum, see Figure 11s in the Supporting Information), 122.3, 122.7 (CH=CH), 124.4, 124.6, 125.3, 126.4, 126.5, 130.6, 130.9 (Ar-CH + CH=CH), 136.6, 136.7, 146.3, 146.7, 146.8, 147.8 (Ar-C), 177.1, 177.3 (NCN), 222.0

(CO). IR (KBr, cm⁻¹): ν = 1964, 1872, 1869, 1848. Anal. Calcd for C₄₀H₄₉AlFeN₄O₅: C, 64.17; N, 7.48; H, 6.60. Found: C, 63.89; N, 7.13; H, 6.83. ESI-HR-MS for [M - 4CO - THP]⁺: calcd *m/z* 637.2416, found *m/z* 637.2475.

(bisNHC)Al(OnBu)[Fe(CO)₄] (6). Compound 3 (0.37 g, 0.5 mmol) was placed in a Schlenk flask (100 mL). THF (50 mL) was transferred to the flask via cannula, and then K[BHR₃] (R = Et, *s*Bu) (0.5 mL, 0.5 mmol, 1 M in THF) was added to the mixture via syringe under vigorous stirring at -20 °C. The mixture was allowed to warm to room temperature and stirred for 12 h. The mixture was filtered, and the obtained filtrate was concentrated to ca. 5 mL and left at -30 °C for 24 h to yield the product 6 as an off-white solid. The product was collected by filtration with a filter funnel, washed with *n*-hexane (5 mL), and dried in vacuo for several hours. Yield: 0.23 g, 0.31 mmol (62%). Mp: 225 °C (dec.). ¹H NMR (400.2 MHz, THF-*d*₈, 298 K, ppm): δ = 0.49–0.55 (m, 7H, CH₃CH₂CH₂CH₂O), 0.99 (d, 6H, CH(CH₃)₂, ³J_{H,H} = 6.8 Hz), 1.00 (d, 6H, CH(CH₃)₂, ³J_{H,H} = 6.8 Hz), 1.12 (d, 6H, CH(CH₃)₂, ³J_{H,H} = 6.6 Hz), 1.33 (d, 6H, CH(CH₃)₂, ³J_{H,H} = 6.8 Hz), 2.29 (sept, 2H, CH(CH₃)₂, ³J_{H,H} = 6.8 Hz), 2.74 (t, 2H, CH₃CH₂CH₂CH₂O), 3.34 (sept, 2H, CH(CH₃)₂, ³J_{H,H} = 6.6 Hz), 6.56 (d, 1H, NCH₂N, ²J_{H,H} = 13.2 Hz), 6.58 (d, 1H, NCH₂N, ²J_{H,H} = 13.2 Hz), 7.17–7.41 (m, 8H, Ar-CH (6H) + CH=CH (2H)), 7.69 (d, 2H, CH=CH, ³J_{H,H} = 1.2 Hz). ¹³C{¹H} NMR (100.2 MHz, THF-*d*₈, 298 K, ppm): δ = 14.7 (OCH₂CH₂CH₂CH₃), 19.4 (OCH₂CH₂CH₂CH₃), 23.5, 24.4, 25.4, 26.2 (CH(CH₃)₂), 28.5, 29.2 (CH(CH₃)₂), 37.3 (OCH₂CH₂CH₂CH₃), 61.6 (OCH₂CH₂CH₂CH₃), 62.3 (NCH₂N), 121.9 (CH=CH), 124.1, 125.1 (Ar-CH), 126.0 (CH=CH), 130.8 (Ar-CH), 136.1 (Ar-C), 146.2, 147.5 (Ar-CN), 222.1 (CO). The ¹³C signal for NCN was not observed in the ¹³C{¹H} NMR spectrum. IR (KBr, cm⁻¹): ν = 1967, 1917, 1860. Anal. Calcd for C₃₉H₄₉AlFeN₄O₅: C, 63.59; N, 7.61; H, 6.70. Found: C, 63.79; N, 7.33; H, 6.85.

[(bisNHC)GaCl₂]⁺Cl⁻ (7). The bisNHC ligand (1) (2.49 g, 5.3 mmol) was dissolved in toluene (50 mL), and the solution was cooled to -78 °C. A solution of GaCl₃ (0.88 g, 5.0 mmol) in toluene (50 mL) was added to the cooled solution of bisNHC via cannula within 10 min under vigorous stirring. A suspension was formed immediately after the addition of GaCl₃, and the obtained mixture was allowed to warm to room temperature and then stirred for another 12 h. The off-white product 7 was obtained by filtration with a filter funnel, washed with *n*-hexane (10 mL) two times, and dried in vacuo for 12 h. Yield: 2.90 g, 4.5 mmol (90%). Mp: 198 °C. A crystal suitable for X-ray diffraction analysis was grown from a saturated CH₂Cl₂ solution at 0 °C. ¹H NMR (200.1 MHz, CD₂Cl₂, 298 K, ppm): δ = 1.06 (d, 12H, CH(CH₃)₂, ³J_{H,H} = 6.8 Hz), 1.17 (d, 12H, CH(CH₃)₂, ³J_{H,H} = 6.8 Hz), 2.35 (sept, 4H, CH(CH₃)₂, ³J_{H,H} = 6.8 Hz), 7.28 (d, 2H, CH=CH, ³J_{H,H} = 1.2 Hz), 7.12–7.41 (m, 4H, Ar-H, except the peaks at 7.32 ppm), 7.49–7.57 (m, 2H, Ar-H), 7.65 (s, 2H, NCH₂N), 8.70 (d, 2H, CH=CH, ³J_{H,H} = 1.8 Hz). ¹³C{¹H} NMR (50.2 MHz, CD₂Cl₂, 298 K, ppm): δ = 23.0, 25.9 (CH(CH₃)₂), 28.9 (CH(CH₃)₂), 60.9 (NCH₂N), 124.7 (CH=CH), 125.5, 125.9 (Ar-CH), 128.5, 129.3 (Ar-C), 131.9 (Ar-CH), 132.2 (Ar-C), 145.7 (Ar-C). The ¹³C signal for NCN was not observed, probably because of coupling with the Ga atom. Anal. Calcd for C₃₁H₄₀Cl₃GaN₄·1/2CH₂Cl₂: C, 55.05; N, 8.15; H, 6.01. Found: C, 55.22; N, 7.76; H, 6.31.

(bisNHC)Ga(Cl)[Fe(CO)₄] (8). Compound 7 (0.33 g, 0.5 mmol) and K₂Fe(CO)₄ (0.11 g, 0.5 mmol) were placed in a Schlenk flask (100 mL) in the glovebox. THF (60 mL) was transferred to the flask via cannula under stirring at -78 °C, and a slightly yellow suspension was formed. The mixture was allowed to warm to room temperature, stirred for another 5 h, and filtered to remove the inorganic precipitate. The obtained light-yellow filtrate was concentrated to ca. 5 mL and left at 0 °C for 12 h to afford compound 8 as a colorless crystalline solid. Yield: 0.25 g, 0.34 mmol (68%). Mp: 246 °C (dec.). Because of the low solubility in commonly used organic solvents (THF, CH₂Cl₂, etc.), all of the attempts to get the NMR spectra of this compound failed. IR (KBr, cm⁻¹): ν = 1992, 1905, 1880, 1847 (CO). Anal. Calcd for C₃₅H₄₀ClFeGaN₄O₄: C, 56.67; N, 7.55; H, 5.44. Found: C, 56.25; N, 7.91; H, 5.66.

(bisNHC)Ga(H)[Fe(CO)₄] (**9**). Compound **8** (0.37 g, 0.5 mmol) was placed in a Schlenk flask (100 mL) in the glovebox. THF (60 mL) was transferred to the flask via cannula to form a light-yellow suspension, and then K[BH(sBu)₃] (0.5 mL, 0.5 mmol, 1 M in THF) was added to the mixture via syringe under vigorous stirring at room temperature. After 12 h of stirring, the mixture was filtered, and the obtained filtrate was concentrated to ca. 5 mL and left at 0 °C for 24 h to afford compound **9** as a colorless-needle crystalline product. The product was collected by decantation of the supernatant and dried in vacuo for several hours. Yield: 0.27 g, 0.38 mmol (76%). Mp: 265 °C (dec.). ¹H NMR (400.2 MHz, THF-*d*₈, 298 K, ppm): δ = 0.98 (d, 6H, CH(CH₃)₂, ³J_{H,H} = 7.2 Hz), 1.03 (d, 6H, CH(CH₃)₂, ³J_{H,H} = 6.8 Hz), 1.21 (d, 6H, CH(CH₃)₂, ³J_{H,H} = 6.8 Hz), 1.30 (d, 6H, CH(CH₃)₂, ³J_{H,H} = 6.4 Hz), 2.54 (sept, 2H, CH(CH₃)₂, ³J_{H,H} = 6.8 Hz), 2.71 (sept, 2H, CH(CH₃)₂, ³J_{H,H} = 6.8 Hz), 4.58 (br, 1H, Ga–H), 6.49 (d, 1H, NCH₂N, ²J_{H,H} = 13.2 Hz), 6.70 (d, 1H, NCH₂N, ²J_{H,H} = 13.2 Hz), 7.20–7.37 (m, 6H, Ar–H), 7.40 (br, 2H, CH=CH), 7.70 (d, 2H, CH=CH, ³J_{H,H} = 1.2 Hz). ¹³C{¹H} NMR (100.2 MHz, THF-*d*₈, 298 K, ppm): δ = 23.3, 23.6, 25.8, 26.4 (CH(CH₃)₂), 28.9, 29.3 (CH(CH₃)₂), 62.6 (NCH₂N), 122.3 (CH=CH), 124.2, 125.3 (Ar–CH), 126.0 (CH=CH), 131.0 (Ar–CH), 135.3 (Ar–C), 145.4, 147.3 (Ar–CN), 181.5 (NCN), 221.6 (CO). IR (KBr, cm^{−1}): ν = 1974, 1887, 1859, 1834 (CO), 1875 (Ga–H). Anal. Calcd for C₃₅H₄₁FeGaN₄O₄: C, 59.43; N, 7.92; H, 5.84. Found: C, 59.79; N, 7.67; H, 5.58.

■ ASSOCIATED CONTENT

■ Supporting Information

Crystal structure of complex **2a**, spectroscopic and crystallographic (CIF) data for **2–9**, and the computational details for the mechanism studies in this paper. This material is available free of charge via the Internet at <http://pubs.acs.org>.

■ AUTHOR INFORMATION

Corresponding Author

matthias.driess@tu-berlin.de

Notes

The authors declare no competing financial interest.

■ ACKNOWLEDGMENTS

We are grateful to the Cluster of Excellence UniCat for financial support (sponsored by the Deutsche Forschungsgemeinschaft and administered by the TU Berlin). S.I. thanks the Alexander von Humboldt Foundation (Sofja Kovalevskaja Program) for financial support. T.S. is thankful for the support of The New Széchenyi Plan TAMOP-4.2.2/B-10/1-2010-0009. We thank Dr. J. D. Epping for help concerning the NMR measurements and Dr. E. Irran for her help with the structure refinement of compound **4**.

■ REFERENCES

- (1) (a) Stephan, D. W. *Org. Biomol. Chem.* **2008**, *6*, 1535–1539. (b) Asay, M.; Jones, C.; Driess, M. *Chem. Rev.* **2011**, *111*, 354–396. (c) Power, P. P. *Nature* **2010**, *463*, 171–177. (d) Mandal, S. K.; Roesky, H. W. *Acc. Chem. Res.* **2012**, *45*, 298–307. (e) Yao, S.; Xiong, Y.; Driess, M. *Organometallics* **2011**, *30*, 1748–1767. (f) Martin, D.; Soleilhavoup, M.; Bertrand, G. *Chem. Sci.* **2011**, *2*, 389–399. (g) Power, P. P. *Chem. Rev.* **2012**, *12*, 238–255.
- (2) (a) Blom, B.; Enthaler, S.; Inoue, S.; Irran, E.; Driess, M. *J. Am. Chem. Soc.* **2013**, *135*, 6703–6713. (b) Rodriguez, R.; Gau, D.; Contie, Y.; Kato, T.; Saffon-Merceron, N.; Baceiredo, A. *Angew. Chem., Int. Ed.* **2011**, *50*, 11492–11495. (c) Hadlington, T. J.; Hermann, M.; Frenking, G.; Jones, C. *J. Am. Chem. Soc.* **2014**, *136*, 3028–3031. (d) Tan, G.; Wang, W.; Blom, B.; Driess, M. *Dalton Trans.* **2014**, *43*, 6006–6011. (e) Jana, A.; Roesky, H. W.; Schulzke, C.; Samuel, P. P. *Organometallics* **2010**, *29*, 4837–4841. (f) Jana, A.; Ghoshal, D.; Roesky, H. W.; Objartel, I.; Schwab, G.; Stalke, D. *J. Am. Chem. Soc.* **2009**, *131*, 1288–1293. (g) Dunn, N. L.; Ha, M.; Radosevich, A. T. *J. Am. Chem. Soc.* **2012**, *134*, 11330–11333. (h) Franz, D.; Inoue, S. *Chem.—Eur. J.* **2014**, DOI: 10.1002/chem.201402293. (i) Franz, D.; Irran, E.; Inoue, S. *Dalton Trans.* **2014**, *43*, 4451–4461. (j) Franz, D.; Inoue, S. *Chem.—Asian. J.* **2014**, DOI: 10.1002/asia.201402233.
- (3) (a) Rivard, E.; Power, P. P. *Dalton Trans.* **2008**, 4336–4343. (b) Al-Rafia, S. M. I.; Malcolm, A. C.; Liew, S. K.; Ferguson, M. J.; Rivard, E. *J. Am. Chem. Soc.* **2011**, *133*, 777–779. (c) Stoelzel, M.; Präsang, C.; Inoue, S.; Enthaler, S.; Driess, M. *Angew. Chem., Int. Ed.* **2012**, *51*, 399–403. (d) Blom, B.; Driess, M.; Gallego, D.; Inoue, S. *Chem.—Eur. J.* **2012**, *18*, 13355–13360. (e) Al-Rafia, S. M. I.; Malcolm, A. C.; McDonald, R.; Ferguson, M. J.; Rivard, E. *Chem. Commun.* **2012**, *48*, 1308–1310. (f) Inoue, S.; Eisenhut, C. *J. Am. Chem. Soc.* **2013**, *135*, 18315–18318. (g) Rivard, E. *Dalton Trans.* **2014**, *43*, 8577–8586.
- (4) Aldridge, S.; Downs, A. J. *Chem. Rev.* **2001**, *101*, 3305–3366.
- (5) (a) Chertihin, G. V.; Andrews, L. *J. Phys. Chem.* **1993**, *97*, 10295–10300. (b) Wang, X.; Andrews, L. *J. Phys. Chem. A* **2003**, *107*, 11371–11379.
- (6) Kinjo, R.; Donnadiou, B.; Celik, M. A.; Frenking, G.; Bertrand, G. *Science* **2011**, *333*, 610–613.
- (7) Fischer, R. A.; Schulte, M. M.; Weiss, J.; Zsolnai, L.; Jacobi, A.; Huttner, G.; Frenking, G.; Boehme, C.; Vyboishchikov, S. F. *J. Am. Chem. Soc.* **1998**, *120*, 1237–1248.
- (8) Wang, Y.; Quillian, B.; Wei, P.; Wannere, C. S.; Xie, Y.; King, R. B.; Schaefer, H. F., III; Schleyer, P. v. R.; Robinson, G. H. *J. Am. Chem. Soc.* **2007**, *129*, 12412–12413.
- (9) Xiong, Y.; Yao, S.; Tan, G.; Inoue, S.; Driess, M. *J. Am. Chem. Soc.* **2013**, *135*, 5004–5007.
- (10) Xiong, Y.; Yao, S.; Inoue, S.; Epping, J. D.; Driess, M. *Angew. Chem., Int. Ed.* **2013**, *52*, 7147–7150.
- (11) (a) Takagi, N.; Shimizu, T.; Frenking, G. *Chem.—Eur. J.* **2009**, *15*, 3448–3456. (b) Takagi, N.; Shimizu, T.; Frenking, G. *Chem.—Eur. J.* **2009**, *15*, 8593–8604.
- (12) Blom, B.; Tan, G.; Enthaler, S.; Inoue, S.; Epping, J. D.; Driess, M. *J. Am. Chem. Soc.* **2013**, *135*, 18108–18120.
- (13) (a) Zlatogorsky, S.; Muryn, C. A.; Tuna, F.; Evans, D. J.; Ingleson, M. J. *Organometallics* **2011**, *30*, 4974–4982. (b) Zlatogorsky, S.; Ingleson, M. J. *Dalton Trans.* **2012**, *41*, 2685–2693.
- (14) Meyer, S.; Orben, C. M.; Demeshko, S.; Dechert, S.; Meyer, F. *Organometallics* **2011**, *30*, 6692–6702.
- (15) Baker, R. J.; Cole, M. L.; Jones, C.; Mahon, M. F. *J. Chem. Soc., Dalton Trans.* **2002**, 1992–1996.
- (16) (a) Stasch, A.; Singh, S.; Roesky, H. W.; Noltemeyer, M.; Schmidt, H.-G. *Eur. J. Inorg. Chem.* **2004**, 4052–4055. (b) Ghadwal, R. S.; Roesky, H. W.; Herbst-Irmer, R.; Jones, P. G. *Z. Anorg. Allg. Chem.* **2009**, *635*, 431–433.
- (17) Cramer, S. A.; Sturgill, F. L.; Chandrachud, P. P.; Jenkins, D. M. *Dalton Trans.* **2014**, *43*, 7687–7690.
- (18) Nagendran, S.; Roesky, H. W. *Organometallics* **2008**, *27*, 457–492.
- (19) Weiss, J.; Stetzkamp, D.; Nuber, B.; Fischer, R. A.; Boehme, C.; Frenking, G. *Angew. Chem., Int. Ed. Engl.* **1997**, *36*, 70–72.
- (20) (a) Lehmann, R.; Schlosser, M. *Tetrahedron Lett.* **1984**, *25*, 745–748. (b) Bates, R. B.; Kroposki, L. M.; Potter, D. E. *J. Org. Chem.* **1972**, *37*, 560–562.
- (21) Kennedy, A. R.; Klett, J.; Mulvey, R. E.; Wright, D. S. *Science* **2009**, *326*, 706–708.
- (22) Crosbie, E.; García-Álvarez, P.; Kennedy, A. R.; Klett, J.; Mulvey, R. E.; Robertson, S. D. *Angew. Chem., Int. Ed.* **2010**, *49*, 9388–9391.
- (23) Armstrong, D. R.; Crosbie, E.; Hevia, E.; Mulvey, R. E.; Ramsay, D. L.; Robertson, S. D. *Chem. Sci.* **2014**, DOI: 10.1039/C4SC01108B.
- (24) (a) Wencel-Delord, J.; Dröge, T.; Liu, F.; Glorius, F. *Chem. Soc. Rev.* **2011**, *40*, 4740–4761. (b) Crabtree, R. H. *J. Chem. Soc., Dalton Trans.* **2001**, 2437–2450. (c) Hashiguchi, B. G.; Bischof, S. M.; Konnick, M. M.; Periana, R. A. *Acc. Chem. Res.* **2012**, *45*, 885–898.
- (25) (a) Deelman, B.-J.; Booij, M.; Meetsma, A.; Teuben, J. H.; Kooijman, H.; Spek, A. L. *Organometallics* **1995**, *14*, 2306–2317.

(b) Holmes, S. M.; Schafer, D. F., II; Wolczanski, P. T.; Lobkovsky, E. B. *J. Am. Chem. Soc.* **2001**, *123*, 10571–10583.

(26) Geier, S. J.; Stephan, D. W. *J. Am. Chem. Soc.* **2009**, *131*, 3476–3477.

(27) We also tried the reduction with KC_8 and sodium naphthalenide, but the reaction afforded only unidentified products.

(28) (a) Marion, N.; Escudero-Adán, E. C.; Benet-Buchholz, J.; Stevens, E. D.; Fensterbank, L.; Malacria, M.; Nolan, S. P. *Organometallics* **2007**, *26*, 3256–3259. (b) Tang, S.; Monot, J.; El-Hellani, A.; Michelet, B.; Guillot, R.; Bour, C.; Gandon, V. *Chem.—Eur. J.* **2012**, *18*, 10239–10243. (c) El-Hellani, A.; Monot, J.; Guillot, R.; Bour, C.; Gandon, V. *Inorg. Chem.* **2013**, *52*, 506–514. (d) Bour, C.; Monot, J.; Tang, S.; Guillot, R.; Farjon, J.; Gandon, V. *Organometallics* **2014**, *33*, 594–599.

(29) (a) Schulte, M. M.; Herdtweck, E.; Raudaschl-Sieber, G.; Fischer, R. A. *Angew. Chem., Int. Ed. Engl.* **1996**, *35*, 424–426.

(b) Fölsing, H.; Segnitz, O.; Bossek, U.; Merz, K.; Winter, M.; Fischer, R. A. *J. Organomet. Chem.* **2000**, *606*, 132–140.

(30) Singh, S.; Ahn, H.-J.; Stasch, A.; Jancik, V.; Roesky, H. W.; Pal, A.; Biadene, M.; Herbst-Irmer, R.; Noltemeyer, M.; Schmidt, H.-G. *Inorg. Chem.* **2006**, *45*, 1853–1860.

(31) Tan, G.; Blom, B.; Gallego, D.; Driess, M. *Organometallics* **2014**, *33*, 363–369.

(32) Sheldrick, G. M. *SHELX-97: Program for Crystal Structure Refinement*; University of Göttingen: Göttingen, Germany, 1997.

(33) Yamashita, M.; Uchida, M.; Tashika, H.; Suemitsu, R. *Bull. Chem. Soc. Jpn.* **1989**, *62*, 2728–2729.